International Communications in Heat and Mass Transfer 38 (2011) 1344–1348

Contents lists available at SciVerse ScienceDirect

International Communications in Heat and Mass Transfer

journal homepage: www.elsevier.com/locate/ichmt

Temperature effects on the effective thermal conductivity of phase change materials with two distinctive phases ☆

X.H. Yang [a], T.J. Lu [b,*], T. Kim [c,*]

[a] School of Energy and Power Engineering, Xi'an Jiaotong University, Xi'an 710049, China
[b] State Key Laboratory for Mechanical Structure Strength and Vibration, School of Aerospace, Xi'an Jiaotong University, Xi'an 710049, China
[c] School of Mechanical Engineering, University of the Witwatersrand, Private Bag 3, Wits 2050, Johannesburg, South Africa

ARTICLE INFO

Available online 9 September 2011

Keywords:
Effective thermal conductivity
Phase change material
Temperature effects
Steady state

ABSTRACT

This study reports on an analytical estimation of the effective thermal conductivity of phase change materials (PCMs) and its dependence upon temperature. During the phase change process, two distinctive phases (solid to liquid) co-exist and the effective thermal conductivity of the PCM varies significantly with temperature. To analytically estimate the variation, the classical Series model assuming one-dimensional (1D) heat conduction normal to the solid–liquid interface was employed. For model validation, experimental measurements with paraffin were conducted covering a wide range of temperature (including the phase change temperature). It was demonstrated that the effective thermal conductivity varies mainly with the fraction of liquid (or solid) phase, bounded by the solid phase conductivity as well as the liquid phase conductivity, whilst the fraction of the liquid phase increased non-linearly with increasing temperature.

1. Introduction

Latent heat storage systems such as heat exchangers with phase change material (PCM), waste heat recovery systems [1], energy-conserving buildings [2] and air-conditioning applications [3] are attractive due to high energy density capabilities during phase change. In such systems, the PCM undergoes phase change by absorbing and releasing heat in an isothermal process. One great advantage of the latent heat storage over other heat dissipation schemes is the compactness of the unit [4].

Amongst the relevant thermal properties of the PCM, the effective thermal conductivity is considered one of the decisive factors in the applications mentioned above. Typically, the PCM has a low thermal conductivity, which limits its wide utilization in heat dissipation applications. Furthermore, the thermal conductivity of the PCM changes depending on its phase. How to quantify it accurately has, therefore, become the focus of numerous recent and past investigations. The bulk thermal conductivity of conventional PCMs (e.g., paraffin) varies with temperature [5–8], particularly when liquid and solid phases co-exist. In practice, unfortunately, the co-existence of two distinctive phases (solid and liquid) is often present in the functioning temperature range. It is, therefore, important to understand how the effective (bulk) thermal conductivity of a PCM is influenced by the presence of the two distinctive phases.

Although many studies have attempted to experimentally quantify the effective thermal conductivity of PCMs [9–12], there is no univocal agreement regarding its variation with temperature in terms of trend and physical mechanism. For example, in the phase change temperature range, whilst Delaunay et al. [10] reported that the effective thermal conductivity has a peak, Inaba et al. [11] argued (based on three data points) that it varies linearly with temperature.

The principal objective of this study is to demonstrate, both theoretically and experimentally, how the effective thermal conductivity of a typical PCM, i.e., paraffin, varies with temperature, covering solid, liquid, and solid–liquid phases. For simplicity, one-dimensional (1D) conduction of heat is assumed in both modeling and experimental measurement. Due to configurational similarities, the classical Series model is employed to estimate analytically the effective thermal conductivity and its dependence upon temperature.

2. Experimental details

2.1. Experimental setup

To measure the steady-state effective thermal conductivity of paraffin in pure solid phase, solid–liquid mixed phase and pure liquid phase, a purposely designed test rig was built as illustrated in Fig. 1. The paraffin melt was poured into a cubic container made of a low conducting material (Perspex). The container had dimensions of 0.14 m (width) × 0.14 m (length) × 0.04 m (height along the *x*-axis), with a wall thickness of 25 mm. Two copper plates with a thermal conductivity of 398 W/(mK) as the substrates were attached to the

☆ Communicated by: P. Cheng and W.Q. Tao.

* Corresponding authors.
E-mail addresses: tjlu@mail.xjtu.edu.cn (T.J. Lu), tong.kim@wits.ac.za (T. Kim).

0735-1933/$ – see front matter © 2011 Elsevier Ltd. All rights reserved.
doi:10.1016/j.icheatmasstransfer.2011.08.021

Nomenclature

c_p	Specific heat of paraffin at constant pressure, $kJ\cdot(kg°C)^{-1}$
Δh_m	Latent heat of paraffin, $kJ\cdot kg^{-1}$
k_s	Thermal conductivity of solid phase of PCM, $W\cdot(mK)^{-1}$
k_f	Thermal conductivity of liquid phase of PCM, $W\cdot(mK)^{-1}$
k_e	Effective thermal conductivity of solid–liquid paraffin, $W\cdot(mK)^{-1}$
L	Total thickness (or length) of PCM parallel to heat flow, m
L_1	Thickness of liquid phase in two-layered system, m
L_2	Thickness of solid phase in two-layered system, m
q''	Heat flux, $W\cdot m^{-2}$
t	Time, s
T_{mean}	Mean temperature of PCM, K
T_m	Melting temperature of PCM, K
T_{p1}	Temperature of paraffin at top surface, K
T_{p2}	Temperature of paraffin at bottom surface, K
T_1	Temperature of upper copper plate at top surface, K
T_2	Temperature of lower copper plate at bottom surface, K
PCM	Phase change material

Greek symbols

α	Thermal diffusivity of paraffin, $m^2\cdot s^{-1}$
ξ	Non-dimensional solid–liquid phase interface location
ρ	Density of paraffin, $kg\cdot m^{-3}$
τ	Non-dimensional time

upper and lower sides of each paraffin sample. A heating element attached to the outer surface of the upper copper plate was controlled by an AC power supply. To minimize heat loss, the side-walls as well as the top and bottom surfaces of the container were covered with a thick thermal insulation material (Fig. 1). To facilitate observing the solid–liquid interface location, a narrow viewing window was machined at the mid-width of the container.

The imposed heat flux q'' normal to the x-axis was measured by a film-type heat flux gauge attached to the central part of the lower copper plate. A T-type foil thermocouple (thickness 13 μm) was also attached to the inner side of the upper copper plate to monitor the surface temperature T_{p1}, and a K-type thermocouple built-in the film heat flux gauge was used to monitor the temperature T_2 (Fig. 1).

The effective thermal conductivity k of the test sample was calculated following Fourier's steady-state heat conduction law, as:

$$k = -\frac{q''L}{\Delta T} \tag{1}$$

where L is the sample length along the x-axis (Fig. 1) and ΔT is the temperature difference between the upper and lower surfaces of the sample:

$$\Delta T = T_{p2} - T_{p1} = T_2 - T_{p1} \tag{2}$$

Here, T_2 is the temperature of the lower surface of the sample, which is assumed to be the same as T_{p2} due to the high conductivity of the copper (substrate) plate.

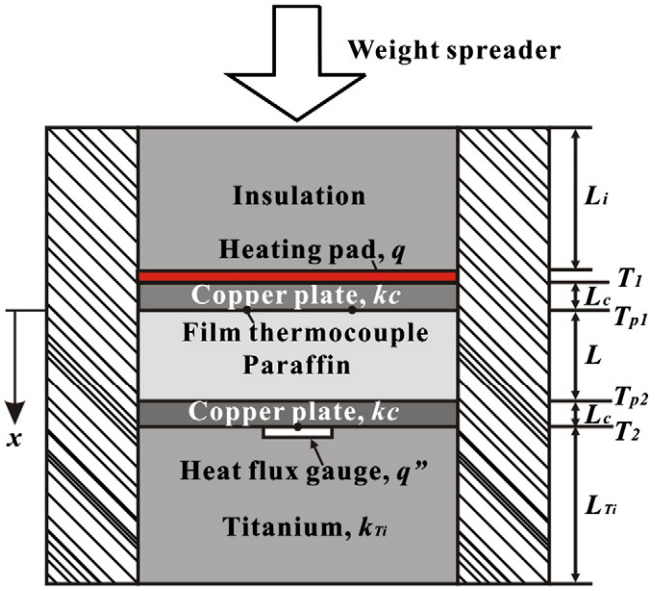

Fig. 1. Schematic of test rig for effective thermal conductivity measurements with controllable power input, with x-axis coinciding with heat flow direction.

2.2. Phase change material

In the present study, paraffin (n-alkane) having a relatively low melting temperature range of 52–54 °C was selected as the target material. To obtain its precise phase change temperature range, a differential scanning calorimeter (DSC) was used and the results were presented in Fig. 2. An evident peak at 54.23 °C representing the intense solid–liquid phase change (solidification) point was observed, and two transition regions corresponding separately to solid-solid (at 40.47 °C) and liquid–liquid (at 60.39 °C) phase transitions were present. In addition, the latent heat of fusion and the melting temperature range were measured to be 102.1 J/g and 40.47 °C–60.39 °C, respectively.

2.3. Thermal conductivity measurement procedures

To minimize the thermal contact resistance between the heat flux gauge and the lower copper plate, mechanical pressure was applied. For paraffin in solid phase, the heat flux was adjusted to ensure that the temperature on the upper copper plate to which the heating

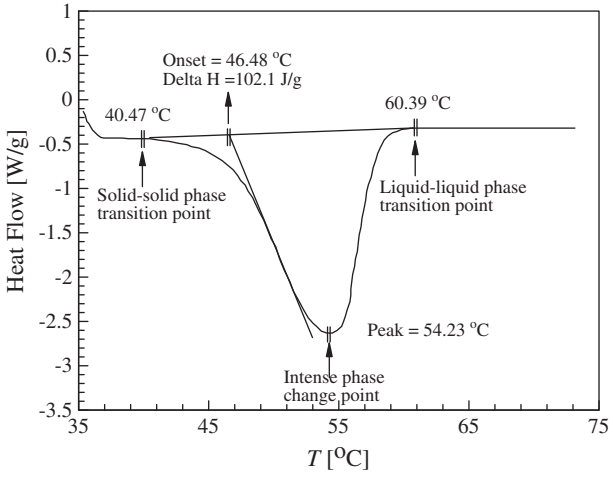

Fig. 2. Differential scanning calorimeter (DSC) measurement results of paraffin used in the present study.

element was attached did not exceed the melting temperature of paraffin. For paraffin in liquid phase, the paraffin melt poured into the cubic container had an initial temperature higher than the melting range (>60.39 °C) and was directly heated without solidifying.

Regarding the thermal conductivity of paraffin in solid–liquid phase, the imposed heat flux level was adjusted so that a stratified mixture with two distinctive layers was obtained. Depending on the heat flux level, the thickness (or depth) of the liquid phase and hence the effective thermal conductivity of the liquid–solid phase varies, upper-bounded by that of the solid phase and lower-bounded by that of the liquid phase. Given that 1D heat conduction was dominant in the present experimental setup, the effective thermal conductivity was calculated by Eq. (1).

During the phase change process, a certain melting/solidifying temperature range (rather than a single temperature value) is present for many PCMs such as polyethylene glycol 600, fluoride salt, chloride eutectic, and paraffin [13,14]. Hence, a proper temperature representing the thermal conductivity of a given PCM needs to be used for its phase transition range. In the present study, following the suggestion of Maglic et al. [15] for steady-state measurements, the arithmetic mean temperature $(T_1+T_2)/2$ was adopted as the representative temperature.

2.4. Measurement uncertainty

Quantifying the thermal conductivity k using the present experimental setup is affected by the following parameters: q'', T_{p1}, T_2, and L. With L fixed at 10 mm, the errors associated with the measurement of k may be estimated as [16]:

$$\frac{\Delta k}{k}=\sqrt{\left(\frac{\Delta q''}{q''}\right)^2+\left(\frac{\Delta T_{p1}}{T_{p1}-T_2}\right)^2+\left(\frac{\Delta T_2}{T_{p1}-T_2}\right)^2} \tag{3}$$

where the error associated with the temperatures T_{p1} and T_2 measured by thermocouples was estimated to be 0.2 °C. The minimum substrate temperature difference (T_{p1}-T_2) was measured to be about 7.3 °C at $q'=203.2$ W/m^2, and the error of the heat flux measured by the heat flux gauge was estimated to be 5.3 W/m^2. Overall, the uncertainty in the present measurement of effective thermal conductivity was estimated to be less than 4.7%.

3. Discussion of results

3.1. Thermal conductivity of PCM in solid and liquid phases

As reference, the thermal conductivity of solid paraffin was measured using the standard hot-disk method, yielding $k_s=0.3129\pm 0.0063$ W/(mK) at 16 °C. Although thermal properties including thermal conductivity vary with the number of carbon atoms in the alkanes, the thermal conductivity of paraffin in both solid and liquid phases is known to be weakly influenced by mean temperature [12] in the range of 10 °C−50 °C, 50 °C being the melting temperature of paraffin tested in the present study.

The thermal conductivity for both the solid and liquid phases of paraffin is considered next. The thermal conductivity was calculated based on the measured temperature difference ΔT defined in Eq. (2) across the total depth L (or length along the x-axis) of the paraffin block, whilst varying the imposed heat flux level q''. Fig. 3 shows the relationship between q'' and $\Delta T/L$, which is linear for both phases. Following the Fourier law (Eq. (1)), the inverse of the slope, $(\Delta T/L)/q''$, is the thermal conductivity. Consequently, the results of Fig. 3 lead to $k_s=0.301$ W/(mK) for the solid phase and $k_f=0.125$ W/(mK) for the liquid phase.

For comparison, the thermal conductivity of solid paraffin was approximately 3.8% lower than that obtained from the hot-disk method.

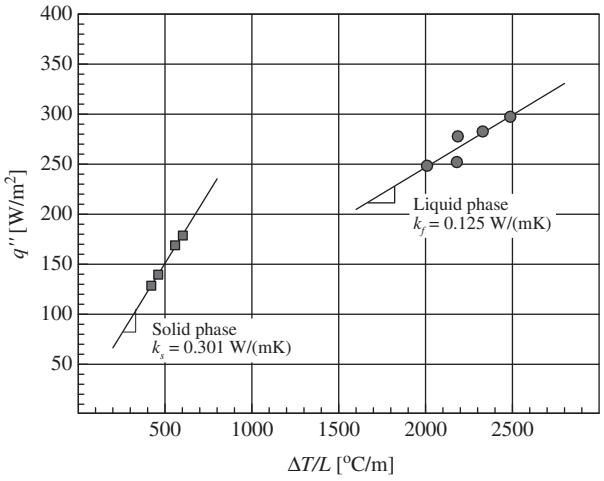

Fig. 3. Temperature difference across both solid and liquid phases of paraffin sample plotted as a function of heating power input.

Liquid paraffin has significantly lower thermal conductivity than solid paraffin, consistent with $k_f=0.126$ W/(mK) reported by Zhang and Zhao [17]. It should be noted that the present configuration of the test setup was designed to minimize the contribution of natural convection in the liquid phase and hence its influence was neglected.

3.2. Thermal conductivity in liquid–solid mixed phase

The effective thermal conductivity k_e of paraffin with two phases mixed having two distinctive layers is considered next. Results from the present experiments plotted in Fig. 4 show the variation of k_e with mean temperature $T_{mean}=(T_1+T_2)/2$ for single (liquid and solid) phases and liquid–solid mixed phase, covering a wide range of mean temperature from 15 °C to 85 °C.

It is seen from Fig. 4 that the effective thermal conductivity is approximately independent of the mean temperature (within the range considered) for paraffin in either solid or liquid phase whereas it varies strongly with the mean temperature in the melting range, $40\ °C\le T_{mean}\le 60\ °C$. Within this range, the effective thermal conductivity lies between k_s (upper bound) and k_f (lower bound), i.e., $k_f\le k_e\le k_s$, decreasing monotonically with increasing T_{mean}. Note that, in contrast to Inaba et al. [11] who conducted experiments on shape-stabilized paraffin, the results of Fig. 4 suggest

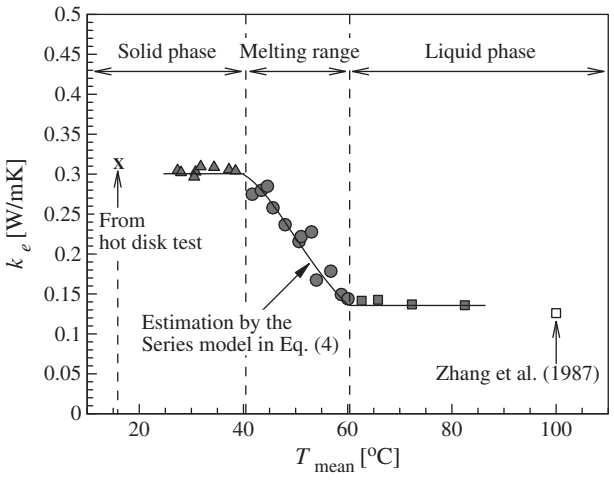

Fig. 4. Dependence of effective thermal conductivity of paraffin on mean temperature.

that the effective thermal conductivity of paraffin varies non-linearly with temperature in the melting range.

To examine analytically how the liquid phase whose thickness increases with increasing mean temperature affects the effective thermal conductivity, the classical Series model of effective thermal conductivity is adopted. The one-dimensional heat flow is normal to the interface between solid and liquid phase layers where T_1 and T_2 are denoted as the temperatures at $x=0$ and $x=L$, respectively, T_m is the melting (phase change) temperature, q'' is the heat flux, and L_1 and L_2 are separately the thickness of liquid and solid layers (see Fig. 1). The Series model suggests that the variation of the effective thermal conductivity in the melting temperature range may be expressed as a function of k_s, k_f and L_1/L as:

$$k_e = \left(\frac{1-L_1/L}{k_s} + \frac{L_1/L}{k_f}\right)^{-1} \tag{4}$$

The phase interface location (or the liquid volume per unit area), L_1, is a function of the mean temperature T_{mean}, as determined below.

With reference to Fig. 1, it is of primary concern that how the temperature at each boundary affects the thickness of the liquidized (or solidified) layer and hence the effective thermal conductivity. This is the so-called "Stefan-type problem" dealing with analytical solutions for the location of phase change interface with limiting boundary conditions [17,18]. For simplicity, the solidification problem under the constant temperature boundary condition having the same configuration was studied first. The non-dimensional solid–liquid interface (ξ) in this case has the form of [18]:

$$\xi = 2\lambda\sqrt{\tau} \tag{5}$$

where τ is a non-dimensional time defined as $\tau=\alpha t/L^2$, λ is the positive root of the following transcendental equation:

$$\lambda\sqrt{\pi}\exp\left(\lambda^2\right)erf(\lambda) = \mathrm{Ste} \tag{6}$$

Here, $erf(\lambda)$ is defined as the Gaussian error function. The Stefan number in this case is defines as $\mathrm{Ste}=c_p(T_m-T_1)/\Delta h_m$ denoting the ratio of sensible heat to the total latent heat in the solidification process.

Fig. 5(a) plots the solidification front ξ as a function of the Stefan number, for non-dimensional time $\tau=1$. It is seen that an increase in the Stefan number (or decrease in T_1) leads to significant thickening of the solidified layer in a nonlinear-monotonic fashion. On the other hand, the melting process considered in this study can be deduced by following the reverse process [20] as illustrated in Fig. 5(a). To experimentally confirm this, the volume of the melting phase per unit area L_1 (or the phase interface location, L_1/L) was measured along the x-axis as a function of the mean temperature T_{mean} (or Stefan number) and results are plotted in Fig. 5(b). The same nonlinear-monotonic trend as that shown in Fig. 5(a) is observed in Fig. 5(b). In the present experiment, the volume of the melting phase per unit area L_1 was measured with constant heat flux, and there were a time-independent temperature T_1 and phase interface location ξ under each steady state, i.e., each steady state corresponds to one constant temperature boundary condition with fixed non-dimensional time τ.

Upon curve-fitting the experimental results of Fig. 5(b), the melting volume per unit area L_1 may be expressed in a quadratic approximation as:

$$L_1 = aT^2_{mean} + bT_{mean} + c \tag{7}$$

where the empirical constants were correlated as $a=0.19714$, $b=-1.4779$ and $c=27.612$. Substitution of Eq. (7) into Eq. (4) enables

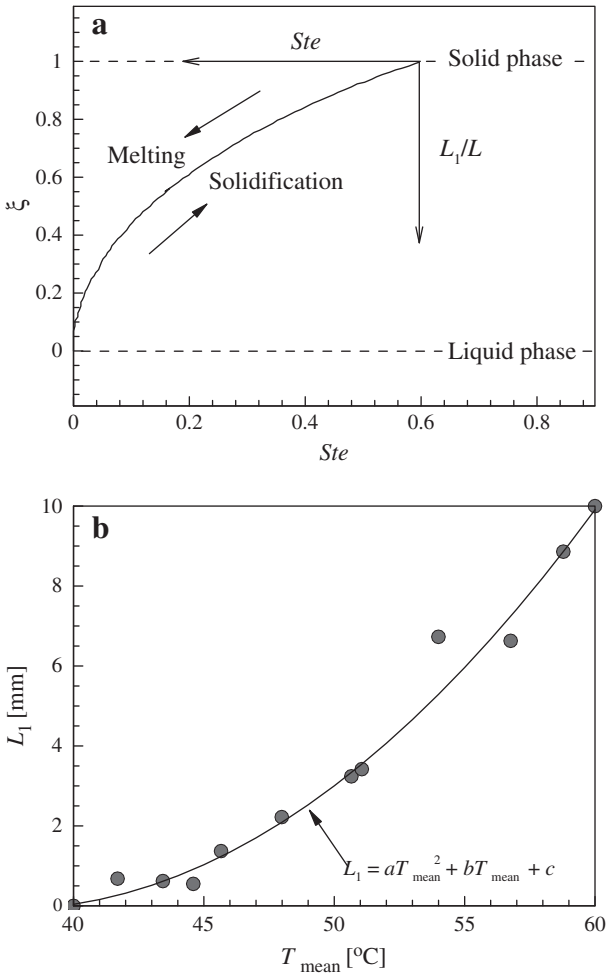

Fig. 5. Variation of liquid–solid interface location with mean temperature: (a) melting (or solidification) front (ξ) plotted as a function of Stefan number for $\tau=1$ [19]; (b) measured one-dimensional liquid volume varying with mean temperature.

one to predict the variation of the effective thermal conductivity of paraffin as a function of mean temperature. The model predictions are included in Fig. 4 along with the present experimental measurements, with excellent agreement achieved. This suggests that the effective thermal conductivity is mainly dependent on the fraction of liquid phase, which increases with increasing mean temperature as empirically correlated in Eq. (7).

Microscopically speaking, at the solid–liquid interface there exist sags and crests, i.e., the so-called "mush" [21], and hence the phase interface macroscopically forms a wavy pattern rather than a single parallel interface line as simplified in the present study. Furthermore, in the present model, the relationship between the volume fraction of liquid phase and the mean temperature was approximated as quadratic and it was assumed that no distinctive liquid layer was present when the temperature slightly exceeded that corresponding to solid–solid transition. Despite these limitations, the observed excellent agreement between the model predictions and the experimental measurements suggests the simplifications and assumptions are reasonable.

4. Conclusions

A simple and yet accurate analytical method for estimating the effective thermal conductivity of phase change materials having two distinctive phases (solid, liquid or liquid–solid mixed phases) was presented. With quasi-steady-state phase change assumed, the

classical Series model was adopted to estimate the effective thermal conductivity of the PCM (paraffin). With the relative volume fraction of the liquid phase approximated as a quadratic function of mean temperature, the dependence of the effective thermal conductivity upon the mean temperature was quantified. The effective thermal conductivity of paraffin in the melting temperature range decreases non-linearly with increasing mean temperature, controlled mainly by the relative volume fraction of the liquid (or solid) phase. Excellent agreement between model predictions and experimental measurements is reached.

Acknowledgements

This study is supported by the National Basic Research Program of China (2011CB610305), the National "111" Project of China (B06024), and the National Natural Science Foundation of China (10825210 and 11072188).

References

[1] A.F. Regin, S.C. Solanki, J.S. Saini, Heat transfer characteristics of thermal energy storage system using PCM capsule: a review, Renewable and Sustainable Energy Reviews 12 (2008) 2438–2458.
[2] R. Baetens, B.P. Jelle, A. Gustavsen, Phase change materials for building applications: a state-of-the-art review, Energy and Buildings 42 (2010) 1361–1368.
[3] S.M. Vakilaltojjar, W. Saman, Analysis and modeling of a phase change storage system for air conditioning applications, Apply Thermal Engineering 23 (2003) 251–283.
[4] B. Liu, P. Majumdar, Numerical simulation of phase change heat transfer in PCM-encapsulated heat sinks, 18th IEEE SEMI-THERM Symposium, 2002, pp. 88–91.
[5] Z. Belén, M.M. José, F.C. Luisa, M. Harald, Review on thermal energy storage with phase change: materials, heat transfer analysis and applications, Apply Thermal Engineering 23 (2003) 251–283.
[6] A.F. Regin, S.C. Solanki, J.S. Saini, An analysis of a packed bed latent heat thermal energy storage system using PCM capsules: numerical investigation, Renewable Energy 34 (2009) 1765–1773.
[7] X. Liu, H. Liu, S. Wang, L. Zhang, H. Cheng, Preparation and thermal properties of form stable paraffin phase change material encapsulation, Journal of Energy Conversion and Management 47 (2006) 2515–2522.
[8] J.M. Marí´n, B. Zalba, L.F. Cabeza, H. Mehling, Improvement of a thermal energy storage using plates with paraffin–graphite composite, International Journal of Heat and Mass Transfer 48 (2005) 2561–2570.
[9] Y.P. Zhang, Y. Jiang, Y. Jiang, A simple method, the T-history method, of determining the heat of fusion, specific heat and thermal conductivity of phase-change materials, Measurement Science and Technology 10 (1999) 201–205.
[10] D. Delaunay, P. Carré, Dispositif de mesure automatique de la conductivité thermique des matériaux à changement de phase, Revue de Physique Appliquée 17 (1982) 209–215.
[11] H. Inaba, P. Tu, Evaluation of thermophysical characteristics on shape-stabilized paraffin as a solid–liquid phase change material, Heat and Mass Transfer 32 (1997) 307–312.
[12] J. Wang, H. Xie, Z. Xin, Thermal properties of paraffin based composites containing multi-walled carbon nanotubes, Thermochimica Acta 488 (2009) 39–42.
[13] A. Sharma, V.V. Tyagi, C.R. Chen, D. Buddhi, Review on thermal energy storage with phase change materials and applications, Renewable and Sustainable Energy Reviews 13 (2009) 318–345.
[14] M.M. Kenisarin, High-temperature phase change materials for thermal energy storage, Renewable and Sustainable Energy Reviews 14 (2010) 955–970.
[15] K.D. Maglic, A. Cezairliyan, V.E. Peletsky, Compendium of thermophysical property measurement methods, Plenum Press, 1984.
[16] H.W. Coleman, W.G. Steele, Experimentation and uncertainty analysis for engineers, 2nd Edition John Wiley & Sons, Inc, 1999.
[17] J.R. Zhang, T.Y. Zhao, A handbook of the thermal properties of working fluid in engineering project, the 1st edition, New Times Press, Beijing, 1987 (in Chinese).
[18] H.S. Carslaw, J.C. Jaeger, Conduction of Heat in Solids, Oxford University Press, Oxford, 1959.
[19] B. Zhang, T. Kim, T.J. Lu, Analytical solution for solidification of close-celled metal foams, International Journal of Heat and Mass Transfer 52 (2009) 133–141.
[20] F. Kreith, F.E. Romie, A study of the thermal diffusion equation with boundary conditions corresponding to solidification or melting of materials initially at the fusion temperature, Proceedings of the Physical Society, Section B 68 (1955) 277–291.
[21] V.R. Voller, C. Prakash, A fixed grid numerical modelling methodology for convection-diffusion mushy region phase-change problems, International Journal of Heat and Mass Transfer 30 (1987) 1709–1719.